

Existence of homoclinic connections in continuous piecewise linear systems

Victoriano Carmona[†] Fernando Fernández-Sánchez[†]
Elisabeth García-Medina[†] Antonio E. Teruel[‡]

Abstract

Numerical methods are often used to put in evidence the existence of global connections in differential systems. The principal reason is that the corresponding analytical proofs are usually very complicated. In this work we give an analytical proof of the existence of a pair of homoclinic connections in a continuous piecewise linear system, which can be considered to be a version of the widely studied Michelson system. Although the

[†]Departamento de Matemática Aplicada II. Universidad de Sevilla. Escuela Superior de Ingenieros. Camino de los Descubrimientos s/n. 41092 Sevilla, España (vcarmona@us.es, fefesan@us.es, egarme@us.es). Partially supported by the *Ministerio de Ciencia y Tecnología, Plan Nacional I+D+I*, in the frame of the projects MTM2006-00847, MTM2007-64193 and by the *Conserjería de Educación y Ciencia de la Junta de Andalucía* (TIC-0130, EXC/2005/FQM-872, P08-FQM-03770).

[‡]Departament de Matemàtiques i Informàtica. Universitat de les Illes Balears. Carretera de Valldemossa km. 7.5. 07122 Palma de Mallorca, España (antonioe.teruel@uib.es). Partially supported by the *MCYT* grant MTM2005-06098-C02-1, by *UIB* grant UIB2005/6 and by *CAIB* grand number CEH-064864.

computations developed in this proof are specific to the system, the techniques can be extended to other piecewise linear systems.

Nowadays, piecewise linear systems are becoming an important tool in the understanding of a wide range of dynamical phenomena in several areas of physics, engineering and sciences in general. In fact, they are being actively studied because they are able to reproduce the richness of behavior found in general nonlinear systems. Among these complex behavior in three-dimensional systems, global connections (in particular, homoclinic orbits) have a relevant role since their presence assure, under certain conditions, the appearance of chaos. However, the proof of the existence of these orbits is generically a difficult task and numerical techniques are often used. In this work, we give an analytical proof of the existence of a symmetrical pair of homoclinic connections in a continuous piecewise linear system. This system can be considered to be a version of the widely studied Michelson system, which appears in the analysis of steady solutions of the Kuramoto-Sivashinsky equation.

1 Introduction

Recently, in work [Carmona et al., 2008], the proof of the existence of a reversible T-point heteroclinic cycle has been given in a continuous piecewise linear system. The used methods are based on the explicit integration of the flow in each linear region of the space of variables and the construction of a system of equations and inequalities that have to be fulfilled by such kind of global bifurcation.

The system studied in work [Carmona et al., 2008],

$$\begin{cases} \dot{x} = y, \\ \dot{y} = z, \\ \dot{z} = 1 - y - c|x|, \end{cases} \quad (1.1)$$

where $c > 0$, can be considered as a continuous piecewise linear version of the well known Michelson system [Freire et al., 2002; Kuramoto et al., 1976; Michelson, 1986; Webster et al., 2003]. In fact, the equations of (1.1) can be obtained from the Michelson system performing a simple linear change of variables followed by the change of function $x^2 \rightarrow |x|$. Moreover, both systems are volume-preserving and time-reversible with respect to the involution $\mathbf{R}(x, y, z) = (-x, y, -z)$. Some other dynamical aspects of the Michelson system also remain in its piecewise linear version [Carmona et al., 2008].

System (1.1) is formed by two linear systems separated by the plane $\{x = 0\}$, called separation plane, and it can be written in a matricial form as

$$\dot{\mathbf{x}} = \begin{cases} A_+ \mathbf{x} + \mathbf{e}_3 & \text{if } x \geq 0, \\ A_- \mathbf{x} + \mathbf{e}_3 & \text{if } x \leq 0, \end{cases} \quad (1.2)$$

with

$$A_+ = \begin{pmatrix} 0 & 1 & 0 \\ 0 & 0 & 1 \\ -c & -1 & 0 \end{pmatrix}, \quad A_- = \begin{pmatrix} 0 & 1 & 0 \\ 0 & 0 & 1 \\ c & -1 & 0 \end{pmatrix} \quad \text{and} \quad \mathbf{e}_3 = \begin{pmatrix} 0 \\ 0 \\ 1 \end{pmatrix}.$$

In the half-space $\{x < 0\}$, the system has exactly one equilibrium point $\mathbf{p}_- = (-1/c, 0, 0)^T$ which is a saddle-focus point. Let $\lambda > 0$ and $\alpha \pm i\beta$ be the eigenvalues of the Jacobian matrix at \mathbf{p}_- . This clearly implies that

$$c = \lambda(1 + \lambda^2), \quad \alpha = -\frac{\lambda}{2}, \quad \beta = \frac{\sqrt{4 + 3\lambda^2}}{2}. \quad (1.3)$$

By the reversibility with respect to \mathbf{R} , there exists exactly one saddle-focus equilibrium $\mathbf{p}_+ = (1/c, 0, 0)^T$ in the half-space $\{x > 0\}$ whose eigenvalues are given by $-\lambda$ and $-\alpha \pm i\beta$.

Using the expression of the parameter c given in (1.3), system (1.1) can be written as

$$\begin{cases} \dot{x} = y, \\ \dot{y} = z, \\ \dot{z} = 1 - y - \lambda(1 + \lambda^2)|x|, \end{cases} \quad (1.4)$$

and the parameter $\lambda > 0$ can be chosen as the fundamental parameter of the family.

Homoclinic connections are orbits that are biasymptotic, for $t \rightarrow \pm\infty$, to the same equilibrium point. The existence of a homoclinic connection to a saddle-focus equilibrium point usually forces a complex dynamical behaviour in a neighbourhood of such connection, see [Gonchenko et al., 1997]. For instance, the celebrated works of Shil'nikov [Shil'nikov, 1965; Shil'nikov, 1970] assure, if a certain eigenvalue ratio condition is satisfied, the existence of infinitely many periodic orbits of saddle type accumulating to the homoclinic cycle.

The proof of the existence of a homoclinic connection is generally a difficult task, even for piecewise linear systems. Some recent works [Wilczak, 2005; Wilczak, 2006] have been devoted to obtain computer-assisted proofs of the existence of global connections in Michelson system. Regarding piecewise linear systems, there are a lot of works about the existence of homoclinic cycles. In many of them [Arneodo et al., 1981; Chua et al., 1986; Couillet et al., 1979; Matsumoto et al., 1985; Matsumoto et al., 1988; Medrano et al., 2005; Medrano et al., 2006] authors require numerical arguments to show that existence. In others [Llibre et al., 2007], authors start from a degenerate situation to avoid any numerical dependence. In the present work we consider a different strategy which can be also used in a generic case.

In the particular case of piecewise linear systems with two zones, homoclinic connections

can be classified attending to the number of intersections with the separation plane. It is obvious that the number of intersections between any homoclinic connection of (1.4) and the separation plane $\{x = 0\}$ has to be greater than one. So, we say that a homoclinic connection of system (1.4) is direct if it intersects the separation plane $\{x = 0\}$ at exactly two points.

The analytical proof of the existence of a pair of direct homoclinic connections will be the main goal of this work, as it is summarized in the following theorem.

Theorem 1.1 *There exists a value $\lambda_h > 1/2$ such that the piecewise linear version (1.4) of the Michelson system has, for $\lambda = \lambda_h$, two direct homoclinic connections, which are symmetric respect to the involution \mathbf{R} .*

Note that, due to the reversibility, if there exists a homoclinic connection Γ of system (1.4), then a new homoclinic connection which can be mapped onto Γ by \mathbf{R} , also exists. Thus, it is only necessary to prove the existence of a direct homoclinic connection Γ to the equilibrium \mathbf{p}_- .

On the other hand, the proof of Theorem 1.1 is partially based on some results of [Carmona et al., 2008] where the boundary value $1/2$, which does not have any dynamical meaning, was chosen for the sake of simplicity of the handmade calculations. In fact, some numerical computations allow to obtain $\lambda_h \approx 0.660759953$.

In Figure 1 the pair of homoclinic connections of (1.4) given by Theorem 1.1 are shown.

The rest of the paper is organized as follows. In section 2 we describe the basic geometric elements of the problem. Section 3 is devoted to the proof of Theorem 1.1, which is divided into two parts. In section 4 we deal with other global connections and show some numerical results.

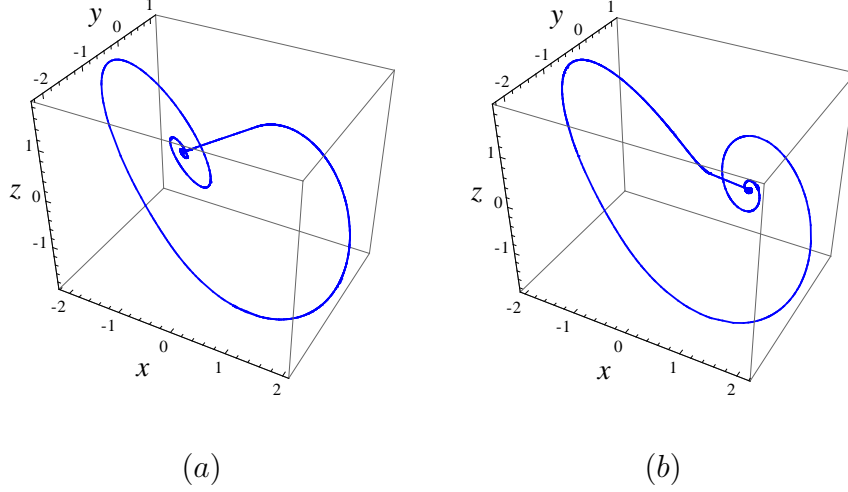


Figure 1: Direct homoclinic orbit to (a) \mathbf{p}_- , (b) \mathbf{p}_+ .

2 Some geometric elements of the flow

In this section we describe the behaviour of the flow crossing the plane $\{x = 0\}$ and the basic elements of the linear dynamics locally contained in the half-spaces $\{x < 0\}$ and $\{x > 0\}$.

For every point $\mathbf{p} = (x_{\mathbf{p}}, y_{\mathbf{p}}, z_{\mathbf{p}})^T \in \mathbb{R}^3$ we denote by $\mathbf{x}_{\mathbf{p}}(t; \lambda) = (x_{\mathbf{p}}(t; \lambda), y_{\mathbf{p}}(t; \lambda), z_{\mathbf{p}}(t; \lambda))^T$ the solution of the system (1.4) with parameter λ and initial condition $\mathbf{x}_{\mathbf{p}}(0; \lambda) = \mathbf{p}$. The corresponding orbit is denoted by $\gamma_{\mathbf{p}}$.

If $x_{\mathbf{p}} = 0$ and $y_{\mathbf{p}} > 0$, then the orbit $\gamma_{\mathbf{p}}$ crosses transversally the plane $\{x = 0\}$ with $x_{\mathbf{p}}(-t; \lambda) < 0$ and $x_{\mathbf{p}}(t; \lambda) > 0$ for $t > 0$ small enough. If $x_{\mathbf{p}}(t; \lambda)$ vanishes in $(0, +\infty)$, then we define the flying time $t_{\mathbf{p}}^+$ as the positive value such that $x_{\mathbf{p}}(t_{\mathbf{p}}^+; \lambda) = 0$ and $x_{\mathbf{p}}(t; \lambda) > 0$ in $(0, t_{\mathbf{p}}^+)$. In such a case, we define the Poincaré map Π_+ at the point \mathbf{p} as $\Pi_+(\mathbf{p}) = \mathbf{x}_{\mathbf{p}}(t_{\mathbf{p}}^+; \lambda)$. Note that the Poincaré map Π_+ only depends on the linear system $\dot{\mathbf{x}} = A_+\mathbf{x} + \mathbf{e}_3$ given in (1.2).

If $x_{\mathbf{p}} = 0$ and $y_{\mathbf{p}} < 0$, then the orbit $\gamma_{\mathbf{p}}$ crosses transversally the plane $\{x = 0\}$ with $x_{\mathbf{p}}(-t; \lambda) > 0$ and $x_{\mathbf{p}}(t; \lambda) < 0$ for $t > 0$ small enough. If $x_{\mathbf{p}}(t; \lambda)$ vanish in $(0, +\infty)$, then we define the flying time $t_{\mathbf{p}}^-$ as the positive value such that $x_{\mathbf{p}}(t_{\mathbf{p}}^-; \lambda) = 0$ and $x_{\mathbf{p}}(t; \lambda) < 0$ in

$(0, t_{\mathbf{p}}^-)$. In such a case, we define the Poincaré map Π_- at the point \mathbf{p} as $\Pi_-(\mathbf{p}) = \mathbf{x}_{\mathbf{p}}(t_{\mathbf{p}}^-; \lambda)$.

This map only depends on the linear system $\dot{\mathbf{x}} = A_- \mathbf{x} + \mathbf{e}_3$.

If \mathbf{p} belongs to the z -axis; i.e. $x_{\mathbf{p}} = 0$ and $y_{\mathbf{p}} = 0$, then \mathbf{p} is called a contact point of the flow of system (1.4) with the plane $\{x = 0\}$ because the vector field at this point is tangent to the plane. Following [Llibre et al., 2004], the first coordinate of the Taylor expansion of $\mathbf{x}_{\mathbf{p}}(t; \lambda) - \mathbf{p}$ at $t = 0$ is

$$\mathbf{e}_1^T (\mathbf{x}_{\mathbf{p}}(t; \lambda) - \mathbf{p}) = z_{\mathbf{p}} \frac{t^2}{2} + \frac{t^3}{3!} + \mathbf{e}_1^T \mathbf{x}_{\mathbf{p}}^{(4)}(\xi; \lambda) \frac{t^4}{4!}.$$

Hence, if $z_{\mathbf{p}} < 0$, then orbit $\gamma_{\mathbf{p}}$ is locally contained in the half-space $\{x \leq 0\}$; if $z_{\mathbf{p}} > 0$, then $\gamma_{\mathbf{p}}$ is locally contained in the half-space $\{x \geq 0\}$; and if $z_{\mathbf{p}} = 0$, then $\gamma_{\mathbf{p}}$ crosses the plane $\{x = 0\}$ from the half-space $\{x < 0\}$ to the half-space $\{x > 0\}$.

Now we describe the basic elements of the linear dynamics in the half-space $\{x < 0\}$, all this information is summarized in Figure 2. The elements in the other half-space can be obtained using the involution \mathbf{R} .

The unstable manifold $W^u(\mathbf{p}_-)$ of \mathbf{p}_- contains the half-line $\mathcal{L}_- = \{\mathbf{p}_- - \mu(1, \lambda, \lambda^2)^T : \frac{-1}{\lambda(1+\lambda^2)} \leq \mu < \infty\}$ generated by the eigenvector associated to the eigenvalue λ of the matrix A_- . The half-line and the plane $\{x = 0\}$ intersect at the point

$$\mathbf{m}_- = \left(0, \frac{1}{1+\lambda^2}, \frac{\lambda}{1+\lambda^2}\right)^T.$$

The stable two-dimensional manifold $W^s(\mathbf{p}_-)$ is locally contained in the half-plane

$$\mathcal{P}_- = \{\lambda(1+\lambda^2)x + \lambda^2y + \lambda z = -1 : x \leq 0\},$$

which is called the focal half-plane of \mathbf{p}_- . This half-plane is obtained from the eigenvectors associated to the complex eigenvalues of A_- . The half-plane \mathcal{P}_- and the separation plane

$\{x = 0\}$ intersect along the straight-line

$$\mathcal{D}_- = \{x = 0, \lambda^2 y + \lambda z = -1\}.$$

Let us emphasize that not every point in \mathcal{D}_- belongs to the stable manifold $W^s(\mathbf{p}_-)$. The intersection point of \mathcal{D}_- and the z -axis is $\mathbf{q}_- = (0, 0, -1/\lambda)^T$. Since \mathbf{q}_- is a contact point, the orbit $\gamma_{\mathbf{q}_-}$ is tangent to the separation plane $\{x = 0\}$ at \mathbf{q}_- . Thus, the segment $\mathcal{S}_- \subset \mathcal{D}_-$ with endpoints \mathbf{q}_- and $\Pi_-^{-1}(\mathbf{q}_-)$ is contained in $W^s(\mathbf{p}_-)$.

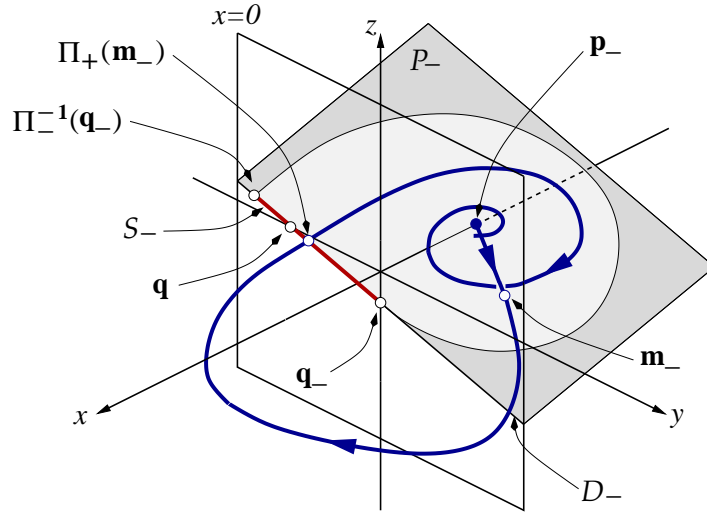


Figure 2: Direct homoclinic connection to \mathbf{p}_- and some geometric elements of the flow.

3 Existence of a direct homoclinic connection to \mathbf{p}_- .

A direct homoclinic orbit to \mathbf{p}_- has to intersect the plane $\{x = 0\}$ at \mathbf{m}_- , since it corresponds to the linear one-dimensional manifold of \mathbf{p}_- . On the other side, this orbit also has to belong to the two-dimensional manifold of \mathbf{p}_- , that is, it has to intersect segment \mathcal{S}_- . Thus, when the condition $\Pi_+(\mathbf{m}_-) \in \mathcal{S}_-$ holds, a direct homoclinic connection to \mathbf{p}_- exists in system (1.4). In

fact, the existence of such homoclinic connection can be derived from conditions

$$\overline{\mathbf{q}\mathbf{q}}_- \subset \mathcal{S}_- \quad (3.1)$$

and

$$\Pi_+(\mathbf{m}_-) \in \overline{\mathbf{q}\mathbf{q}}_-, \quad (3.2)$$

where $\mathbf{q} = (0, -1/\lambda^2, 0)$ is the intersection point of the straight lines \mathcal{D}_- and \mathcal{D}_+ , see Figure 2.

As a corollary of Proposition 3.3 in [Carmona et al., 2008], it follows that there exists a value $\lambda^* \in (0, 1/2)$ such that for every $\lambda \geq \lambda^*$ condition (3.1) is satisfied. On the other hand, since the orbit through \mathbf{m}_- cannot intersect the focal plane \mathcal{P}_+ , it is easy to conclude that $\Pi_+(\mathbf{m}_-) \in \overline{\mathbf{q}\mathbf{q}}_-$ if and only if $\Pi_+(\mathbf{m}_-) \in \mathcal{D}_-$. In other words, conditions (3.1) and (3.2) are equivalent to the existence of $t_h > 0$ and $\lambda_h > 1/2$ such that $\mathbf{x}_{\mathbf{m}_-}(t_h, \lambda_h) \in \mathcal{D}_-$ and $x_{\mathbf{m}_-}(t, \lambda_h) > 0$ for every $t \in (0, t_h)$. It is obvious that if a such a pair (t_h, λ_h) exists, then $\mathbf{x}_{\mathbf{m}_-}(t_h, \lambda_h)$ has to satisfy the system

$$\begin{cases} x_{\mathbf{m}_-}(t, \lambda) = 0, \\ \lambda^2 y_{\mathbf{m}_-}(t, \lambda) - \lambda z_{\mathbf{m}_-}(t, \lambda) + 1 = 0, \end{cases} \quad (3.3)$$

obtained by integrating, for $x > 0$, system (1.4) with initial condition $\mathbf{x}(0, \lambda) = \mathbf{m}_-$.

Now, the proof of condition (3.2) is divided into two parts. First, we establish that system (3.3) has a solution (t_h, λ_h) with $t_h > 0$ and $\lambda_h > 1/2$. Secondly, we check that $x_{\mathbf{m}_-}(t, \lambda_h) > 0$ for every $t \in (0, t_h)$.

After some algebra, system (3.3) leads to the following equivalent system

$$\begin{cases} E_1(t, \lambda) = 0, \\ E_2(t, \lambda) = 0, \end{cases} \quad (3.4)$$

where

$$E_1(t, \lambda) = 2\lambda^2 e^{\frac{3\lambda}{2}t} \left[\sqrt{4 + 3\lambda^2} \cos(\beta t) - 3\lambda \sin(\beta t) \right] + \sqrt{4 + 3\lambda^2} \left[(1 + \lambda^2) - (1 + 3\lambda^2)e^{\lambda t} \right], \quad (3.5)$$

$$E_2(t, \lambda) = 2\lambda^2 e^{\frac{3\lambda}{2}t} \left[\sqrt{4 + 3\lambda^2} \cos(\beta t) + \lambda \sin(\beta t) \right] + \sqrt{4 + 3\lambda^2} (1 + \lambda^2) e^{\lambda t}, \quad (3.6)$$

and β is defined in expression (1.3).

The curves defined by the equations of system (3.4) are shown in Figure 3. It is possible to see that they intersect in several points. This is a numerical evidence of the existence of solutions (t, λ) , with $t > 0$ and $\lambda > 0$, for this system. In what follows, an analytical proof of the existence of the first intersection point (corresponding to the smallest value of $t > 0$) is derived.

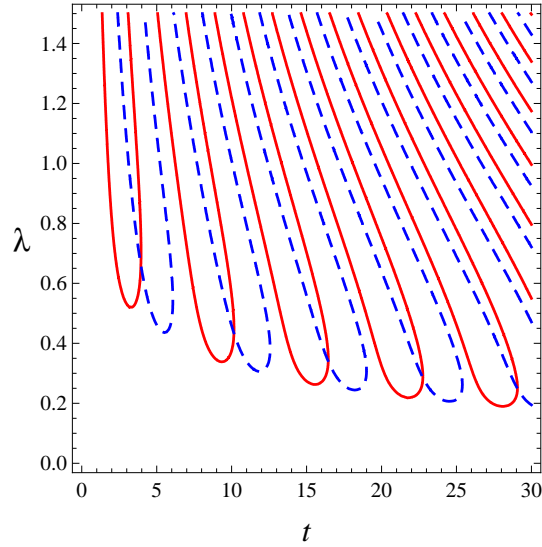


Figure 3: Dashed curves are given by equation $E_1(t, \lambda) = 0$ and solid ones correspond to equation $E_2(t, \lambda) = 0$.

Taking into account the relative position of the curves given by the equations of system (3.4) it is convenient to manipulate these equations to get a more suitable system. Adding $e^{\lambda t}(1 + \lambda^2)$

times (3.5) to $[e^{\lambda t}(1 + 3\lambda^2) - (1 + \lambda^2)]$ times (3.6) and dividing by $2\lambda^2 e^{\frac{3\lambda}{2}t}$ gives

$$E(t, \lambda) = \sqrt{4 + 3\lambda^2} [2(1 + 2\lambda^2)e^{\lambda t} - (1 + \lambda^2)] \cos(\beta t) - \lambda [2e^{\lambda t} + 1 + \lambda^2] \sin(\beta t) = 0. \quad (3.7)$$

From (3.4) the trigonometric functions are given by

$$\begin{aligned} \sin(\beta t) &= -\frac{\sqrt{4 + 3\lambda^2} [2(1 + 2\lambda^2)e^{\lambda t} - (1 + \lambda^2)] e^{-\frac{3\lambda}{2}t}}{8\lambda^3}, \\ \cos(\beta t) &= -\frac{(1 + \lambda^2 + 2e^{\lambda t}) e^{-\frac{3\lambda}{2}t}}{8\lambda^2}. \end{aligned} \quad (3.8)$$

Note that both functions are strictly negative for $t > 0$ and $\lambda > 0$.

It is now obvious that

$$\sin^2(\beta t) + \cos^2(\beta t) = \frac{e^{-3\lambda t}}{64\lambda^4} \left[\frac{(4 + 3\lambda^2) [2(1 + 2\lambda^2)e^{\lambda t} - (1 + \lambda^2)]^2}{\lambda^2} + (1 + \lambda^2 + 2e^{\lambda t})^2 \right]$$

or, equivalently,

$$\frac{e^{-3\lambda t}}{64\lambda^4} \left[\frac{(4 + 3\lambda^2) [2(1 + 2\lambda^2)e^{\lambda t} - (1 + \lambda^2)]^2}{\lambda^2} + (1 + \lambda^2 + 2e^{\lambda t})^2 \right] - 1 = 0.$$

Simplifying this equation gives

$$p(t, \lambda) = -16\lambda^6 e^{3\lambda t} + (1 + \lambda^2)^2 [4(1 + 3\lambda^2)e^{2\lambda t} - 2(2 + 3\lambda^2)e^{\lambda t} + 1 + \lambda^2] = 0. \quad (3.9)$$

Note that a solution (t, λ) of system (3.4) also satisfies the system given by equations (3.7) and (3.9). However, as it is established in Lemma 3.1, another condition is necessary for the converse to be true: the sinus function in (3.8) must always be negative for $t > 0$ and $\lambda > 0$.

In Figure 4 the curves given by equations (3.7) and (3.9) and the sign of the sinus function in (3.8) are shown. Comparing with Figure 3, note that there exist intersection points between the curves which are not solutions of system (3.4).

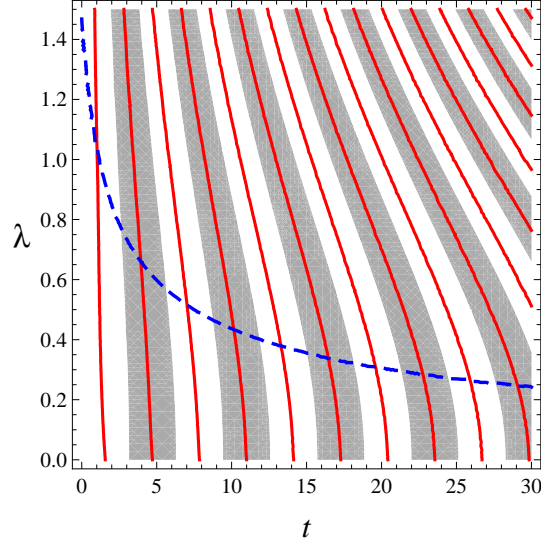


Figure 4: Solid curves are given by equation (3.7) and the dashed one corresponds to equation (3.9). The set where $\sin(\beta t) < 0$ is shaded.

Lemma 3.1 *For $t > 0$ and $\lambda > 0$, system (3.4) is equivalent to the system*

$$\begin{cases} E(t, \lambda) = 0, \\ p(t, \lambda) = 0, \\ \sin(\beta t) < 0. \end{cases} \quad (3.10)$$

Proof. The first part of the equivalence, that is, the proof that a solution (t, λ) of system (3.4) with $t > 0$ and $\lambda > 0$ also satisfies the system (3.10), is direct.

For the other implication, let us consider the system

$$\begin{cases} -\sqrt{4 + 3\lambda^2} [2(1 + 2\lambda^2)e^{\lambda t} - (1 + \lambda^2)] X + \lambda [2e^{\lambda t} + (1 + \lambda^2)] Y = 0, \\ X^2 + Y^2 - 1 = 0, \end{cases} \quad (3.11)$$

which represents the intersection in coordinates (X, Y) of a straight line with positive slope containing the origin and the unit circle. Obviously, system (3.11) has a unique solution which negative second coordinate.

Note that

$$(X_1, Y_1) = \left(-\frac{(2e^{\lambda t} + 1 + \lambda^2) e^{-\frac{3\lambda}{2}t}}{8\lambda^2}, -\frac{\sqrt{4 + 3\lambda^2} [2(1 + 2\lambda^2)e^{\lambda t} - (1 + \lambda^2)] e^{-\frac{3\lambda}{2}t}}{8\lambda^3} \right)$$

is a solution of system (3.11) whose second coordinate is negative for $t > 0$ and $\lambda > 0$.

On the other hand, if (t, λ) is a solution of system (3.4) with $t > 0$ and $\lambda > 0$, then

$$(X_2, Y_2) = (\sin(\beta t), \cos(\beta t))$$

is also a solution of system (3.11) whose second coordinate is negative.

Therefore, we conclude that $(X_1, Y_1) = (X_2, Y_2)$ with $t > 0$ and $\lambda > 0$. Since this equality corresponds to system (3.8), which is equivalent to system (3.4), the lemma holds. ■

Now let us proof that system (3.10) has at least a solution.

Lemma 3.2 *System (3.3) has a solution (t_h, λ_h) in the open set*

$$\Omega = \left\{ (t, \lambda) \in \mathbb{R}^2 : \frac{2\pi}{\sqrt{4 + 3\lambda^2}} < t < \frac{4\pi}{\sqrt{4 + 3\lambda^2}}, \quad \frac{1}{2} < \lambda < \sqrt{3} \right\}.$$

Proof. From lemma 3.1 it is known that systems (3.3) and (3.10) are equivalent for $t > 0$ and $\lambda > 0$.

Since the third condition of (3.10) is satisfied for every $(t, \lambda) \in \Omega$ it is only necessary to show that system

$$\begin{cases} E(t, \lambda) = 0, \\ p(t, \lambda) = 0, \end{cases} \quad (3.12)$$

has solution in Ω . This is, as it is going to be proved, a consequence of Poincaré–Miranda theorem [Kulpa, 1997], which can be considered as a n -dimensional extension of Bolzano theorem.

The change of variables $\mu = \lambda^2$, $\tau = \sqrt{4 + 3\lambda^2} t/2$ transforms system (3.12) into the system

$$\begin{cases} \tilde{E}(\tau, \mu) = E\left(\frac{2\tau}{\sqrt{4+3\mu}}, \sqrt{\mu}\right) = 0, \\ \tilde{p}(\tau, \mu) = p\left(\frac{2\tau}{\sqrt{4+3\mu}}, \sqrt{\mu}\right) = 0, \end{cases} \quad (3.13)$$

and Ω into $\tilde{\Omega} = (\pi, 2\pi) \times (1/4, 3)$.

From the definition of E it is obvious that $\tilde{E}(\pi, \mu) > 0$ and $\tilde{E}(2\pi, \mu) < 0$ for $\mu \geq 0$. Thus, function \tilde{E} takes different signs at the vertical sides of the boundary of $\tilde{\Omega}$.

In order to analyze the sign of function \tilde{p} at the horizontal sides of the boundary of $\tilde{\Omega}$, let us define

$$P(s, \mu) = -16\mu^3 s^3 + (1 + \mu)^2 [4(1 + 3\mu)s^2 - 2(2 + 3\mu)s + 1 + \mu], \quad (3.14)$$

which corresponds to function \tilde{p} when

$$s = \exp\left(\sqrt{\mu} \frac{2\tau}{\sqrt{4 + 3\mu}}\right) \geq 1. \quad (3.15)$$

Since the derivative of $P(s, 3)$ with respect to s is negative in \mathbb{R} and $P(1, 3) < 0$, we have $P(s, 3) < 0$ for $s \geq 1$. Therefore, $\tilde{p}(\tau, 3) < 0$ for every $\tau \in [\pi, 2\pi]$.

For the last side of the rectangle, straightforward computations show that the derivative of $P(s, 1/4)$ is positive in $[1, 27]$. Taking into account that $P(1, 1/4) = \frac{259}{64}$ it follows that $P(s, 1/4)$ is positive for every $s \in [1, 27]$.

Note that, from (3.15), if $\mu = 1/4$ and $\tau \in [\pi, 2\pi]$, then $s \in [1, 27]$. Thus, $\tilde{p}(\tau, 1/4)$ is positive for $\tau \in [\pi, 2\pi]$.

The lemma follows by the Poincaré–Miranda theorem. ■

At this moment we have proved that there exists a point $(t_h, \lambda_h) \in \Omega$ such that $\mathbf{x}_{\mathbf{m}_-}(t_h, \lambda_h) \in \mathcal{D}_-$. For condition (3.2) to be fulfilled it is also necessary to prove that $x_{\mathbf{m}_-}(t, \lambda_h) > 0$ for every $t \in (0, t_h)$. The next result deals with this inequality.

Lemma 3.3 *If $(t_h, \lambda_h) \in \Omega$ is a solution of system (3.10), then $x_{\mathbf{m}_-}(t, \lambda_h) > 0$ for every $t \in (0, t_h)$.*

Proof. According to the equations of system (1.4), the derivative with respect to t of function $x_{\mathbf{m}_-}(t, \lambda_h)$ is given by $y_{\mathbf{m}_-}(t, \lambda_h)$. By integrating this system for $x > 0$, we obtain

$$\dot{x}_{\mathbf{m}_-}(t, \lambda_h) = y_{\mathbf{m}_-}(t, \lambda_h) = c_1 e^{-\lambda_h t} + e^{\frac{\lambda_h}{2}t} \left[c_2 \cos \left(\frac{\sqrt{4 + 3\lambda_h^2}}{2} t \right) + c_3 \sin \left(\frac{\sqrt{4 + 3\lambda_h^2}}{2} t \right) \right], \quad (3.16)$$

where

$$c_1 = \frac{1}{1 + 3\lambda_h^2} > 0, \quad c_2 = \frac{2\lambda_h^2}{(1 + 3\lambda_h^2)(1 + \lambda_h^2)} > 0, \quad c_3 = \frac{2\lambda_h(2 + 3\lambda_h^2)}{(1 + 3\lambda_h^2)(1 + \lambda_h^2)\sqrt{4 + 3\lambda_h^2}} > 0.$$

On one hand, note that $x_{\mathbf{m}_-}(0, \lambda_h) = 0$ and $\dot{x}_{\mathbf{m}_-}(0, \lambda_h) > 0$. On the other hand, let us assume that $(t_h, \lambda_h) \in \Omega$ is a solution of system (3.10). Therefore, $x_{\mathbf{m}_-}(t_h, \lambda_h) = 0$. Substituting (3.8) in (3.16) it is obvious that

$$\dot{x}_{\mathbf{m}_-}(t_h, \lambda_h) = y_{\mathbf{m}_-}(t_h, \lambda_h) = \frac{-2 + e^{-\lambda_h t_h}}{2\lambda_h^2} < 0.$$

Let us also assume that there exists a value $\hat{t} \in (0, t_h)$ such that $x_{\mathbf{m}_-}(\hat{t}, \lambda_h) = 0$. Then, $y_{\mathbf{m}_-}(t, \lambda_h)$ must vanish in at least three values in $(0, t_h)$, that is, the equation

$$h(\tau) = e^{\frac{3\lambda_h}{\sqrt{4+3\lambda_h^2}}\tau} \left[\frac{c_2}{c_1} \cos(\tau) + \frac{c_3}{c_1} \sin(\tau) \right] = -1,$$

which is obtained from $y_{\mathbf{m}_-}(t, \lambda_h) = 0$, has to vanish in at least three values in $(0, 2\pi)$.

Since $h(0) = c_2/c_1 > 0$, equation $h(\tau) = 0$ must have at least three solutions in $(0, 2\pi)$, what is not possible. Thus, function $x_{\mathbf{m}_-}(t, \lambda_h)$ cannot vanish in $(0, t_h)$ and the proof is concluded.

■

4 Other global connections

In the previous sections, the existence of a pair of direct homoclinic connections, which are symmetric respect to the involution \mathbf{R} , has been proved for $\lambda = \lambda_h \approx 0.660759953$. The first

step of this proof is the analysis of the solutions of the system (3.10). Those solutions are the intersections of the solid and dashed curves of Figure 4 which lie in the shadow regions. Besides the first intersection, which corresponds to the value λ_h , we can observe that other intersections exist.

The second intersection point corresponds to $(t_H, \lambda_H) \approx (10.15402101, 0.43391236)$. It can be also proved that a pair of direct homoclinic connections, which are symmetric respect to the involution \mathbf{R} , exist for λ_H . Remember that the existence of a intersection point is not the only condition that has to be fulfilled to assure the existence of a homoclinic connection; it is also necessary to check that the orbit with initial condition \mathbf{m}_- does not intersect the separation plane for $t \in (0, t_H)$ and $\mathbf{x}_{\mathbf{m}_-}(t_H, \lambda_H)$ belongs to \mathcal{S}_- . As a comparison with the first pair of homoclinic orbits, these second homoclinic connections give an extra loop around the one-dimensional manifold of the other equilibrium. The homoclinic connection to \mathbf{p}_- is shown in Figure 5.

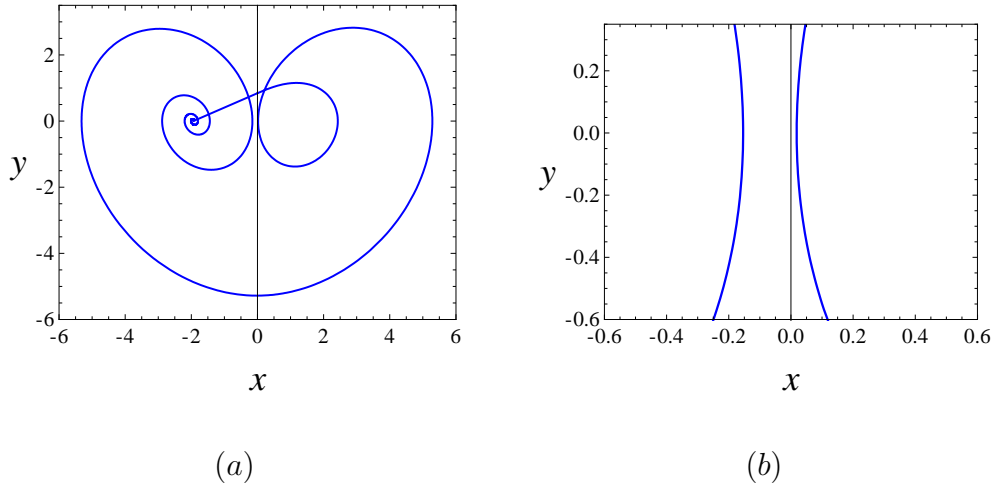


Figure 5: (a) Projection onto the plane xy of a direct homoclinic orbit with a second loop to \mathbf{p}_- . (b) Zoom of (a), where it is clear that the second loop does not intersect $x = 0$.

Regarding to the remainder intersection points in Figure 4, they do not correspond with real

direct homoclinic connections: although each one of them is a solution (t', λ') of system (3.10), the orbit with initial condition \mathbf{m}_- intersects the separation plane for values of $t \in (0, t')$.

This behavior is similar for reversible T-point heteroclinic cycles in system (1.4). In [Carmona et al., 2008], the existence of a “direct” reversible T-point heteroclinic cycle was proved for $\lambda \approx 0.65153556$. This cycle is called direct in the sense that its heteroclinic orbit corresponding to the one-dimensional manifolds has exactly three intersections with the separation plane (which is the minimum possible number of intersections) while the heteroclinic orbit corresponding to the two-dimensional manifolds has only one intersection. Moreover, the existence of another direct reversible T-point heteroclinic cycle can be proved for $\lambda \approx 0.43327834$. This cycle has two extra loops around the one-dimensional manifolds of the equilibria, see Figure 6.

A first step in the proof of the existence of these reversible T-point heteroclinic cycles is the analysis of the existence of solution of a system analogous to (3.10) (given by equations (4.3) and (4.6) in [Carmona et al., 2008]). Besides the values of λ given in the previous paragraph, there exist other solutions of the system which, as the homoclinic case, do not correspond with real reversible T-point heteroclinic cycles.

References

- A. Arneodo, P. Coulet and C. Tresser, “Possible new strange attractors with spiral structure”, *Comm. Math. Phys.* **79**, 573–579 (1981).
- V. Carmona, F. Fernández-Sánchez and A. E. Teruel, “Existence of a reversible T-point heteroclinic cycle in a piecewise linear version of the Michelson system”, *SIAM J. Applied Dynamical Systems*, **7**, 1032–1048 (2008).

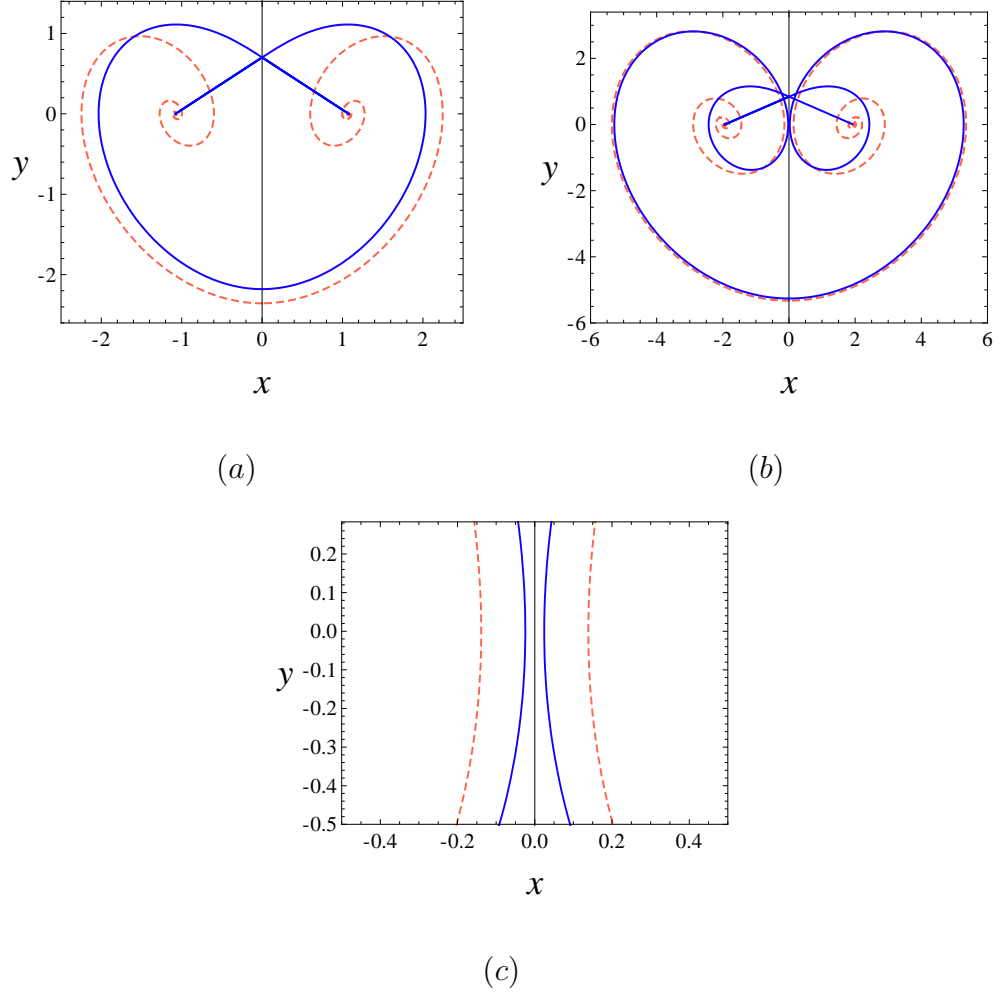


Figure 6: Projections onto the plane xy of the direct T-point heteroclinic cycles which exist for (a) $\lambda \approx 0.65153556$ and (b) $\lambda \approx 0.43327834$. In each figure, the solid curve corresponds to the one-dimensional manifolds of the equilibria while the dashed one is a transversal intersection of the two-dimensional manifolds. (c) Zoom of (b), where it is clear that the small loops do not intersect $x = 0$.

L. O. Chua, M. Komuro and T. Matsumoto, “The double scroll family. II. Rigorous analysis of bifurcation phenomena”, IEEE Trans. Circuits and Systems **33**, 1097–1118 (1986).

P. Couillet, C. Tresser and A. Arneodo, “Transition to stochasticity for a class of forced oscillators”, Phys. Lett. A **72**, 268–270 (1979).

- E. Freire, E. Gamero, A. J. Rodriguez-Luis and A. Algaba, “A note on the triple-zero linear degeneracy: normal forms, dynamical and bifurcation behaviors of an unfolding”, *Internat. J. Bifur. Chaos Appl. Sci. Engrg.* **12**, 2799–2820 (2002).
- S. V. Gonchenko, D. V. Turaev, P. Gaspard and G. Nicolis, “Complexity in the bifurcation structure of homoclinic loops to a saddle-focus”, *Nonlinearity* **10**, 409–423 (1997).
- S. Ibañez and J. A. Rodriguez, “Shil’nikov configurations in any generic unfolding of the nilpotent singularity of codimension three on \mathbb{R}^3 .”, *J. Differential Equations* **208**, 147–175 (2005).
- W. Kulpa, “The Poincaré–Miranda theorem”, *Amer. Math. Monthly* **6**, 545–550 (1997).
- Y. Kuramoto and T. Tsuzuki, “Persistent propagation of concentration waves in dissipative media far from thermal equilibrium”, *Prog. Theoret. Phys.* **55**, 356–369 (1976).
- J. Llibre and A. E. Teruel, “Existence of Poincaré maps in piecewise linear differential systems in \mathbb{R}^n ”, *Internat. J. Bifur. Chaos Appl. Sci. Engrg.* **8**, 2843–2851 (2004).
- J. Llibre, E. Ponce and A. E. Teruel, “Horseshoes near homoclinic orbits for piecewise linear differential systems in \mathbb{R}^3 ”, *Internat. J. Bifur. Chaos Appl. Sci. Engrg.* **17**, 1171–1184 (2007).
- T. Matsumoto, L. O. Chua and M. Komuro, “The double scroll”, *IEEE Trans. Circuits and Systems* **32**, 797–818 (1985).
- T. Matsumoto, L. O. Chua and K. Ayaki, “Reality of chaos in the double scroll circuit: a computer-assisted proof”, *IEEE Trans. Circuits and Systems* **35**, 908–925 (1988).

R. O. Medrano-T., M. S. Baptista and I. L. Caldas, “Basic structures of the Shilnikov homoclinic bifurcation scenario”, *Chaos* **15**, 033112–10 (2005).

R. O. Medrano-T., M. S. Baptista and I. L. Caldas, “Shilnikov homoclinic orbit bifurcations in the Chua’s circuit”, *Chaos* **16**, 043119–9 (2006).

D. Michelson, “Steady solutions of the Kuramoto–Sivashinsky equation”, *Phys. D* **19**, 89–111 (1986).

L. P. Shil’nikov, “A case of the existence of a denumerable set of periodic motions”, *Sov. Math. Dokl.* **6**, 163–166 (1965).

L. P. Shil’nikov, “A contribution to the problem of the structure of an extended neighbourhood of a rough equilibrium state of saddle-focus type”, *Math. USSR Sbornik* **10**, 91–102 (1970).

K. N. Webster and J. N. Elgin, “Asymptotic analysis of the Michelson system”, *Nonlinearity* **16**, 2149–2162 (2003).

D. Wilczak, “Symmetric heteroclinic connections in the Michelson system: a computer assisted proof”, *SIAM J. Appl. Dyn. Syst.* **4**, no. 3, 489–514 (2005).

D. Wilczak, “The existence of Shilnikov homoclinic orbits in the Michelson system: a computer assisted proof”, *Found. Comput. Math.* **6**, no. 4, 495–535 (2006).